Electronic Supplementary Material (ESI) for Nanoscale Advances.

Supporting Information

PdPtRu nanocages with tunable compositions for boosting methanol oxidation reaction

Zihan Leng,[a] Xingqiao Wu,[a] Xiao Li,[a] Junjie Li,[a] Ningkang Qian,[a] Liang Ji,[a] Deren Yang,[a] Hui Zhang[a,b]*

[a]State Key Laboratory of Silicon Materials and School of Materials Science and Engineering, Zhejiang University, Hangzhou, Zhejiang 310027, People's Republic of China.

[b]Institute of Advanced Semiconductors, Hangzhou Innovation Center, Zhejiang University, Hangzhou, Zhejiang 310027, People's Republic of China.

Table S1. ICP-AES data of the PdPtRu nanocages with different compositions.

Samples	**Pt/Pd/Ru atom ratio**	**wt% of Pt**
$PdPt_{2.5}Ru_{2.4}$	2.5:1:2.4	42.4
$PdPt_{7.3}Ru_{3.6}$	7.3:1:3.6	61.3
$PdPt_{3.7}Ru_{8.1}$	3.7:1:8.1	28.9

Table S2. EDX data of the PdPtRu nanocages with different compositions.

Elements	**$PdPt_{2.5}Ru_{2.4}$**	**$PdPt_{7.3}Ru_{3.6}$**	**$PdPt_{3.7}Ru_{8.1}$**
Pt (%)	41.50	60.65	28.69
Ru (%)	40.89	30.89	63.53
Pd (%)	17.61	8.46	7.78
Overall (%)	100.00	100.00	100.00

Table S3. ECSA, specific activity and mass activity of three PdPtRu nanocages, including commercial PtRu/C and Pt/C catalysts.

Samples	**ECSA (m^2/g_{Pt}) -CV curves**	**i_s (mA/cm^2)**	**i_m ($mA/\mu g_{Pt}$)**	**ECSA (m^2/g_{Pt}) - CO stripping**
$PdPt_{2.5}Ru_{2.4}$	59.4	8.20	0.75	62.1
$PdPt_{7.3}Ru_{3.6}$	67.5	5.04	0.38	-
$PdPt_{3.7}Ru_{8.1}$	64.4	4.11	0.29	-
Pt/C	47.6	2.67	0.21	49.6
PtRu/C	42.8	4.95	0.28	44.5

Table S4. Comparison of MOR activities of PdPtRu nanocages in this work with state of art electrocatalysts in the literatures.

Samples	Electrolyte	i_s (mA/cm^2)	i_m (mA/μg$_{Pt}$)	Ref.
$PdPt_{2.5}Ru_{2.4}$ nanocages	0.1 M $HClO_4$+0.5 M CH_3OH	8.2	0.75	This work
CuNi@Pt-Cu nano-polyhedra/C	0.1 M $HClO_4$+1.0 M CH_3OH	5.57	0.66	1
$Pt_{47}Rh_8Cu_{45}$/C	0.1 M $HClO_4$+1.0 M CH_3OH	1.22	0.38	2
PtRu NWs	0.1 M $HClO_4$+0.5 M CH_3OH	1.16	0.82	3
PtRu nanodendrites	0.1 M $HClO_4$+1.0 M CH_3OH	10.08	1.08	4
Pt_5PdCu_5 hexapods	0.5 M H_2SO_4+ 0.5 M CH_3OH	7.39	0.97	5
PtNi CNCs	0.5 M H_2SO_4+ 0.5 M CH3OH	1.37	0.70	6
PtCo/EG	0.5 M H_2SO_4+ 1.0 M CH3OH	0.94	0.53	7
PtCu nanostars	0.5 M H_2SO_4+ 1.0 M CH3OH	3.45	0.574	8
PtFeCu	0.5 M H_2SO_4+ 0.5 M CH3OH	1.783	0.622	9
PtPdCu Nanodendrites	0.5 M H_2SO_4+ 0.5 M CH3OH	0.693	0.52	10
Au@PtCu nanostars	0.1 M $HClO_4$+ 1.0 M CH_3OH	1.06	0.178	11

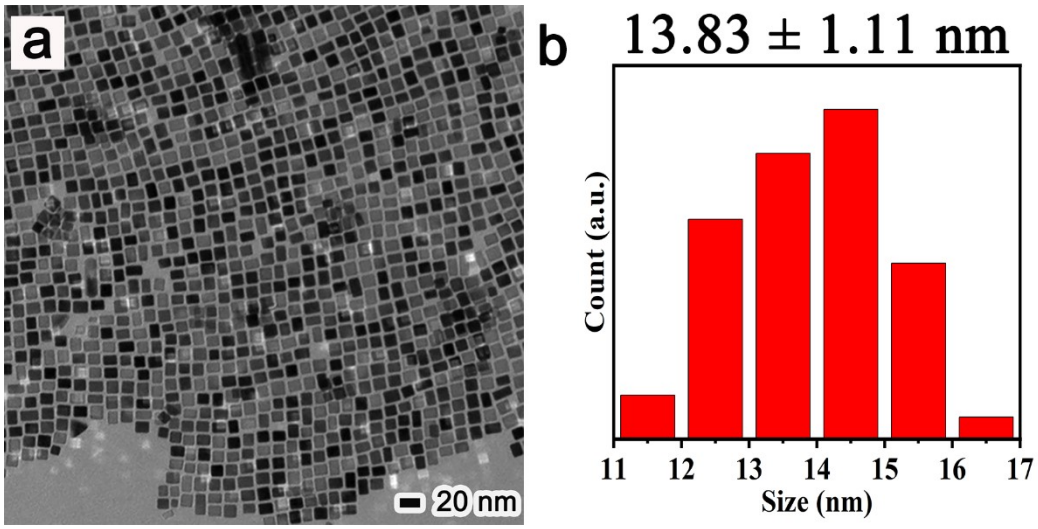

Figure S1. (a) TEM image and (b) size distribution of the Pd nanocubes.

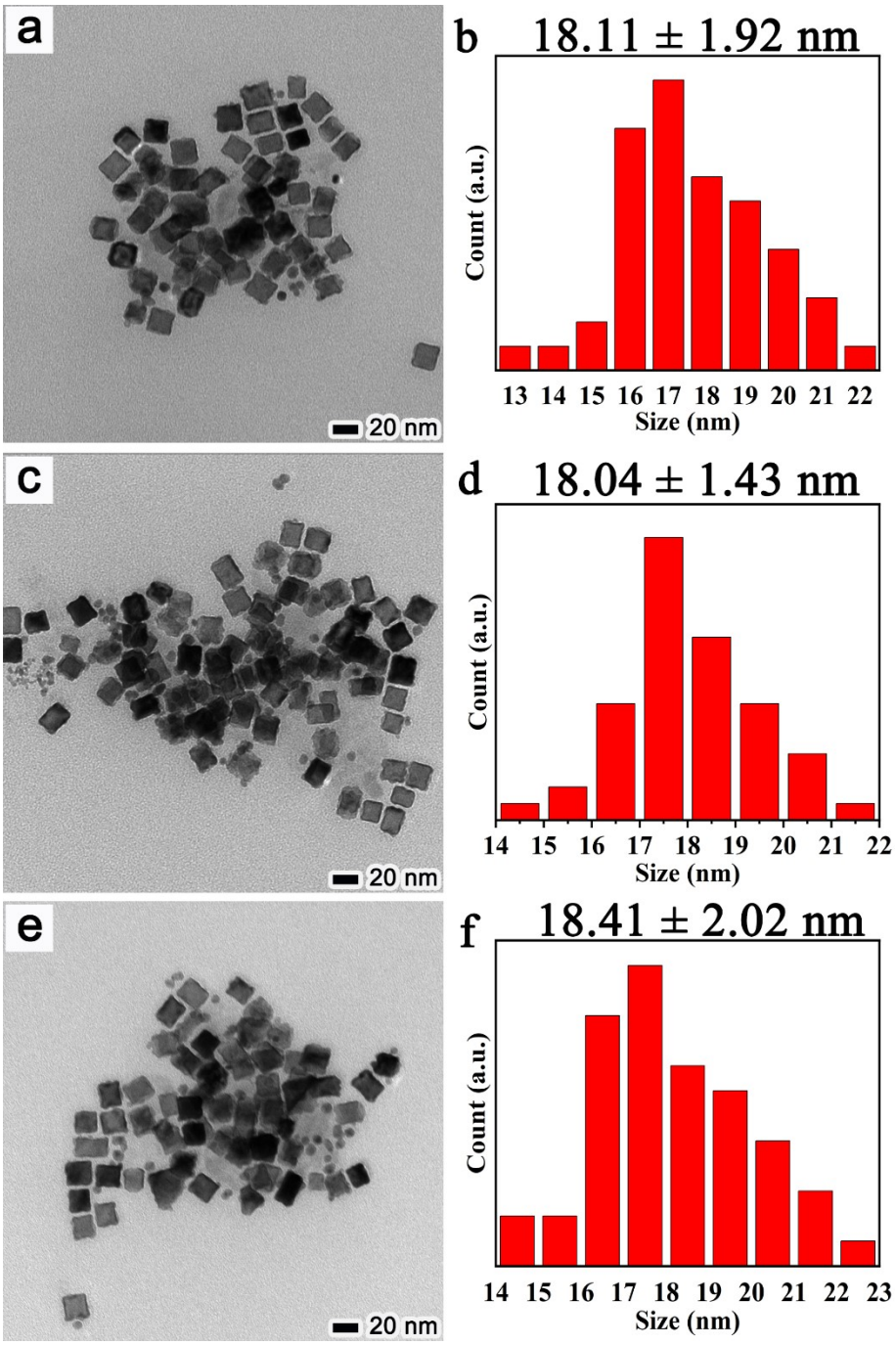

Figure S2. (a, c, e) TEM images and (b, d, f) size distributions of the Pd@PtRu nanocubes prepared using the standard procedure by varying the amount of Pt salt precursors from 0.002 to 0.0015 and 0.001 mmol and Ru salt precursors from 0.001 to 0.0015 and 0.002 mmol, respectively.

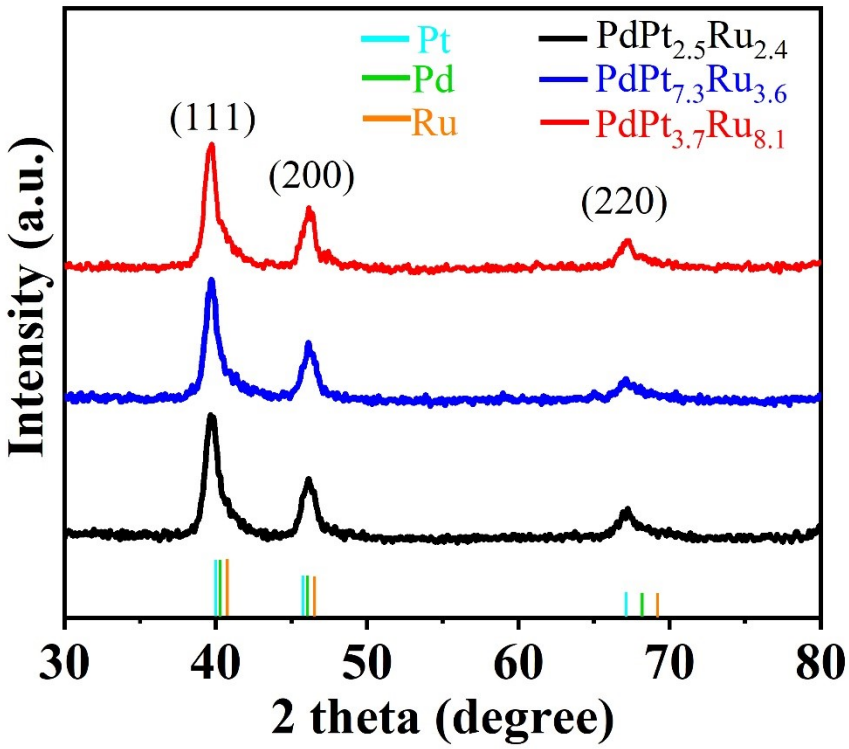

Figure S3. XRD patterns of the as-synthesized nanocubes which were used to synthesize $PdPt_{7.3}Ru_{3.6}$, $PdPt_{2.5}Ru_{2.4}$ and $PdPt_{3.7}Ru_{8.1}$ nanocages.

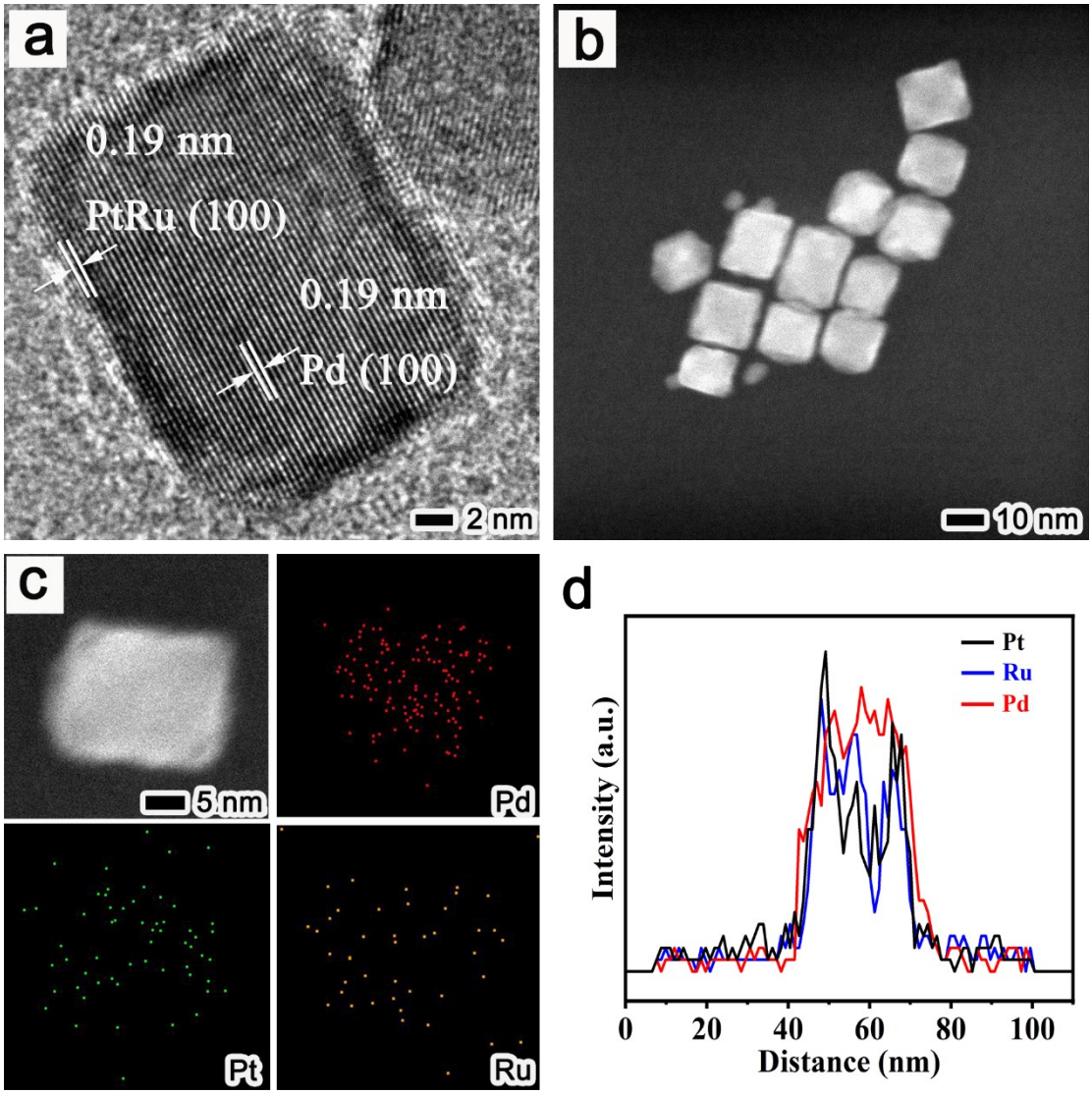

Figure S4. Morphological, structural, and compositional characterizations of the Pd@PtRu nanocages: (a) HRTEM image, (b) HAADF-STEM image, (c) EDX mapping image, and (d) line-scan profiles.

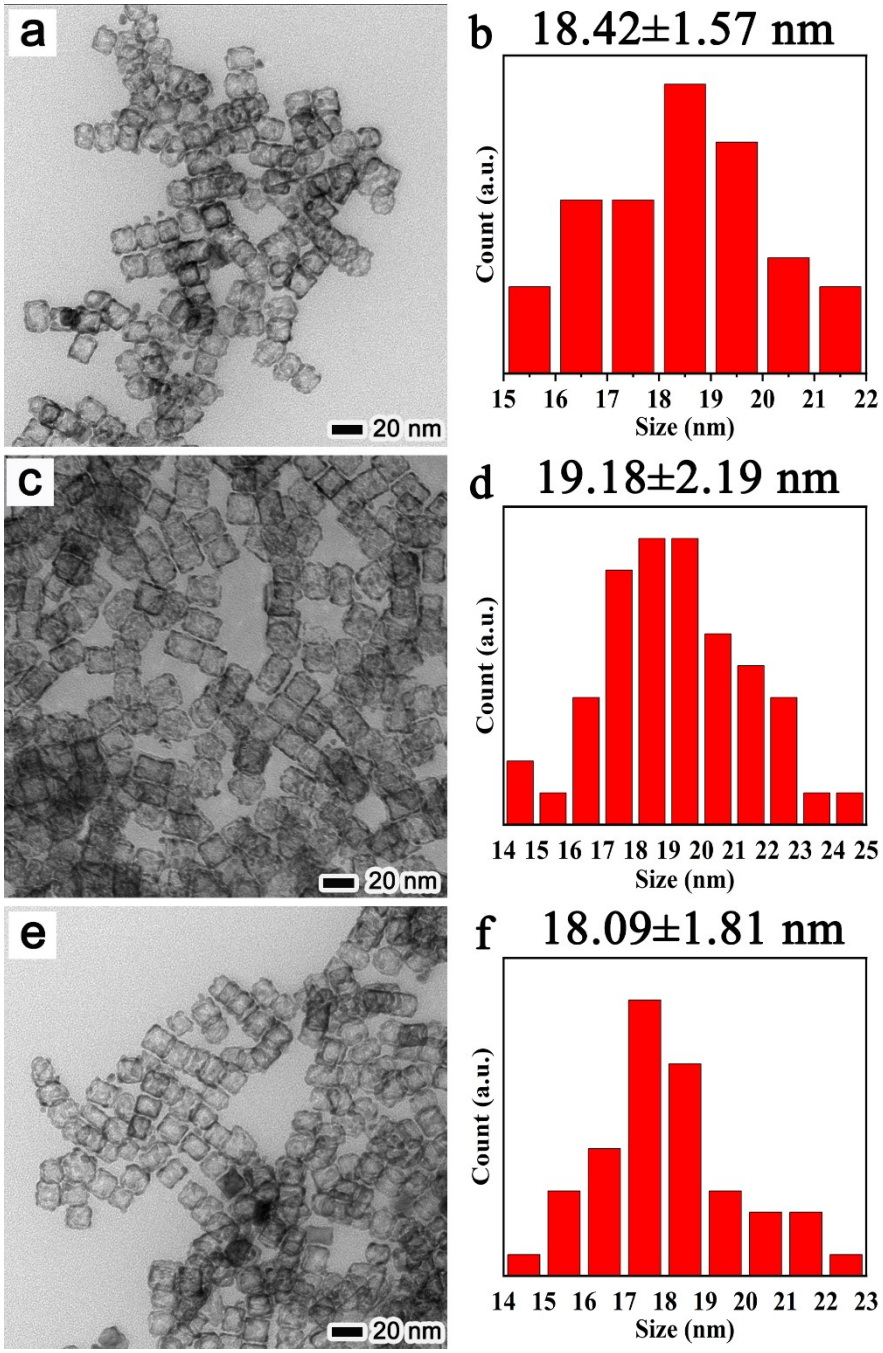

Figure S5. (a, c, e) TEM images and (b, d, f) size distributions of the $PdPt_{2.5}Ru_{2.4}$ nanoframes prepared using the standard procedure by varying the amount of Pt salt precursors from 0.002 to 0.0015 and 0.001 mmol and Ru salt precursors from 0.001 to 0.0015 and 0.002 mmol, respectively.

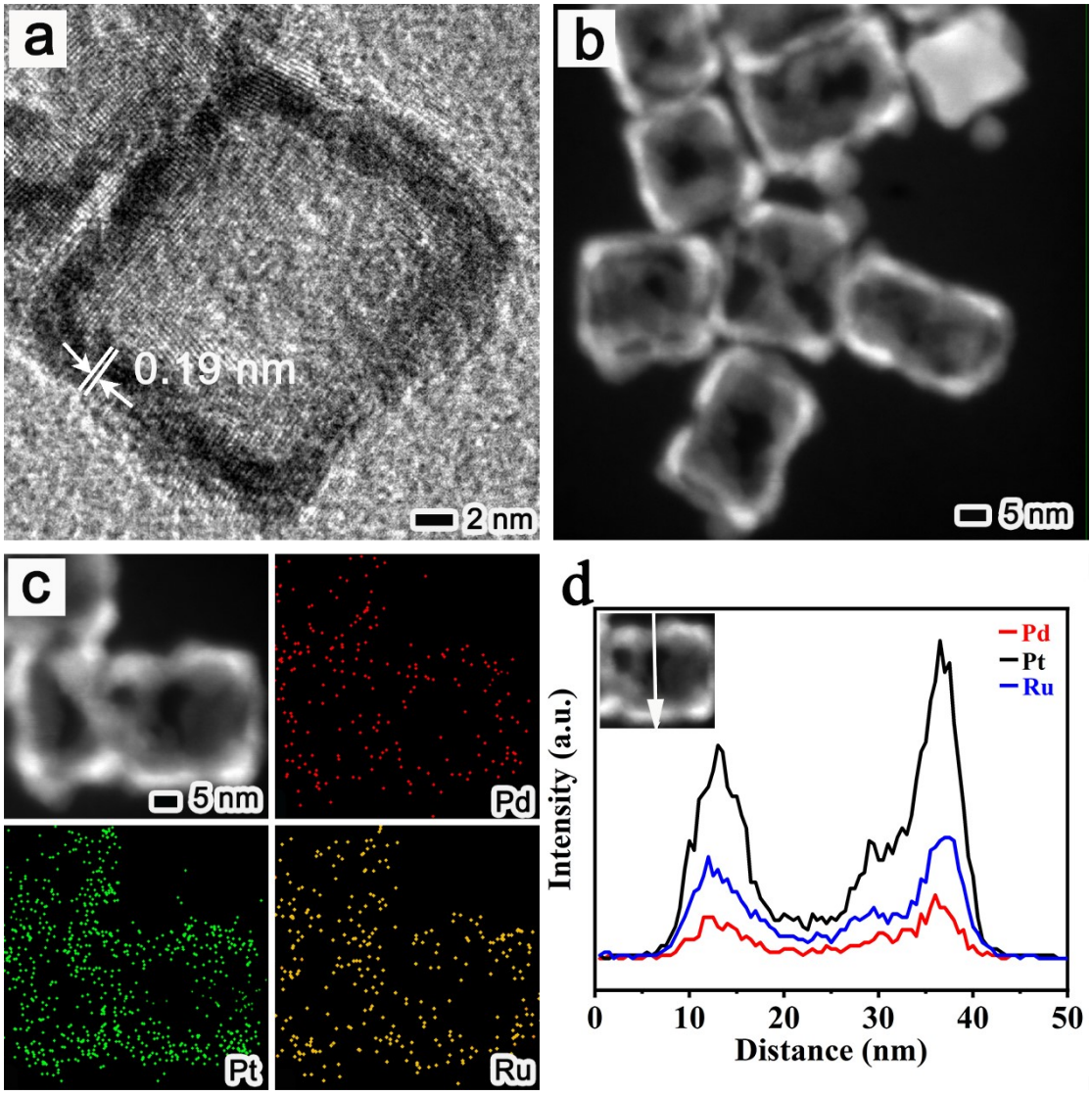

Figure S6. Morphological, structural, and compositional characterizations of the PdPt7.3Ru3.6 nanocages: (a) HRTEM image, (b) HAADF-STEM image, (c) EDX mapping image, and (d) line-scan profiles.

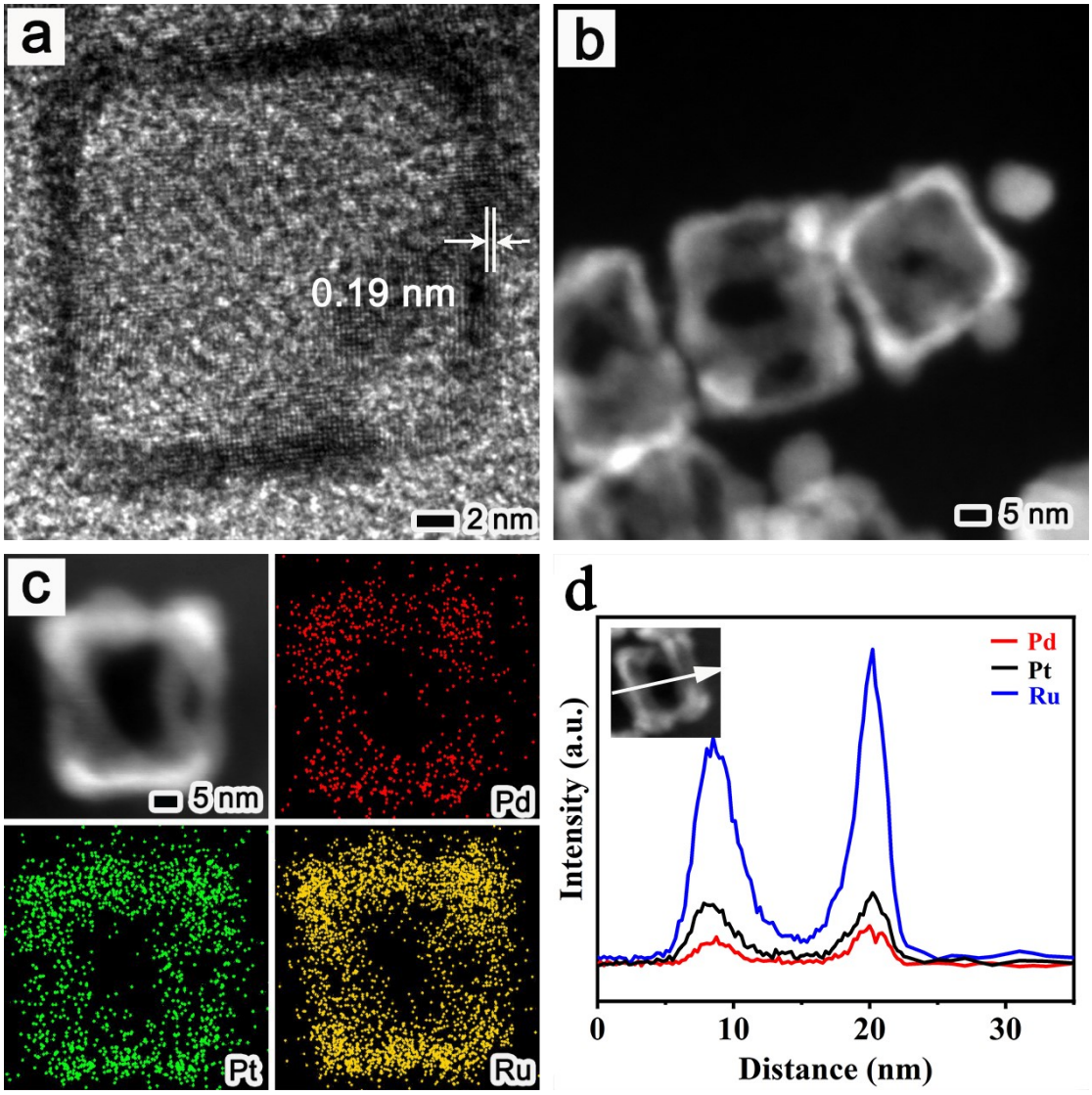

Figure S7. Morphological, structural, and compositional characterizations of the $PdPt_{3.7}Ru_{8.1}$ nanocages: (a) HRTEM image, (b) HAADF-STEM image, (c) EDX mapping image, and (d) line-scan profiles.

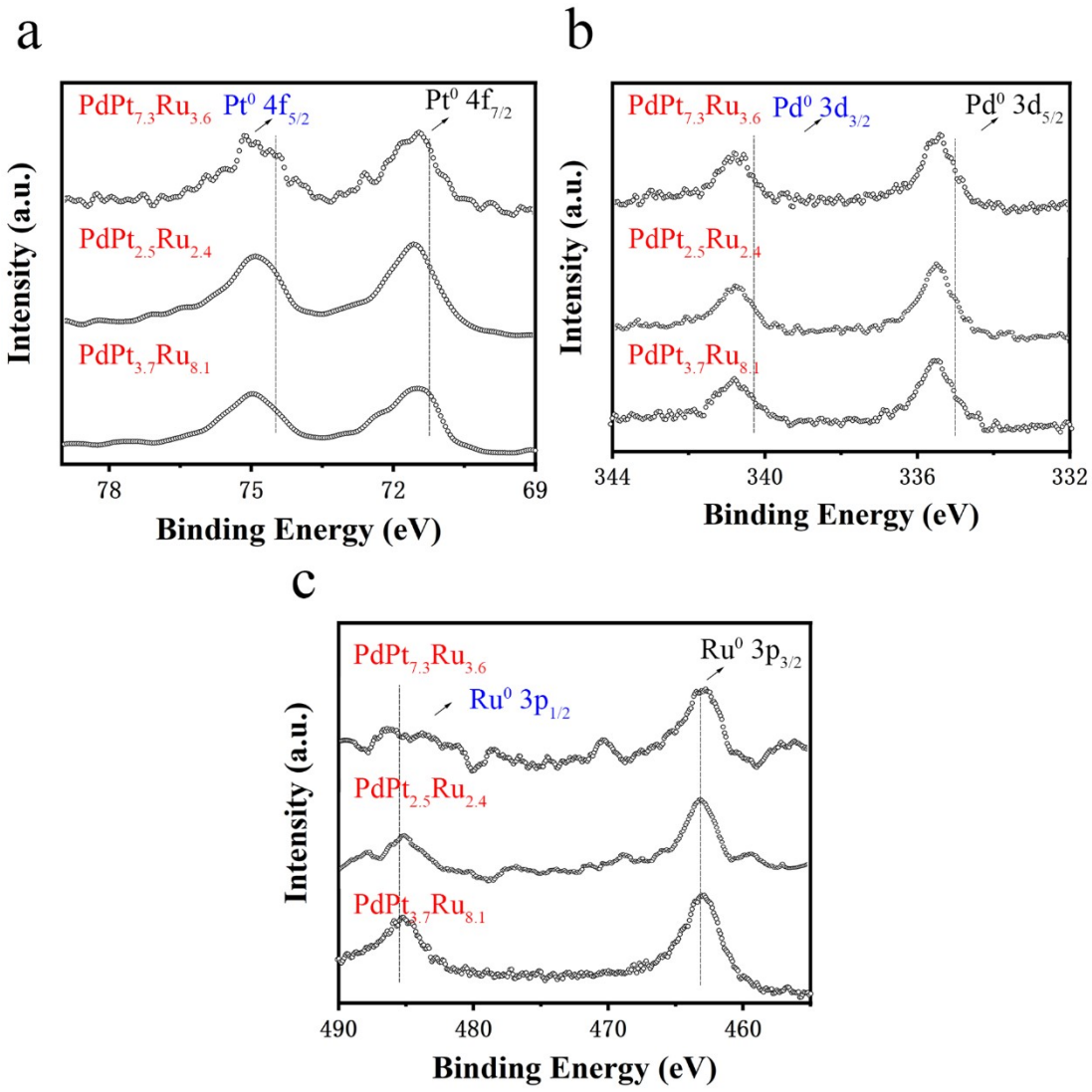

Figure S8. The XPS spectra of the $PdPt_{2.5}Ru_{2.4}$, $PdPt_{7.3}Ru_{3.6}$ and $PdPt_{3.7}Ru_{8.1}$ nanocages for the Pt 4f, Pd 3d and Ru 3p orbitals.

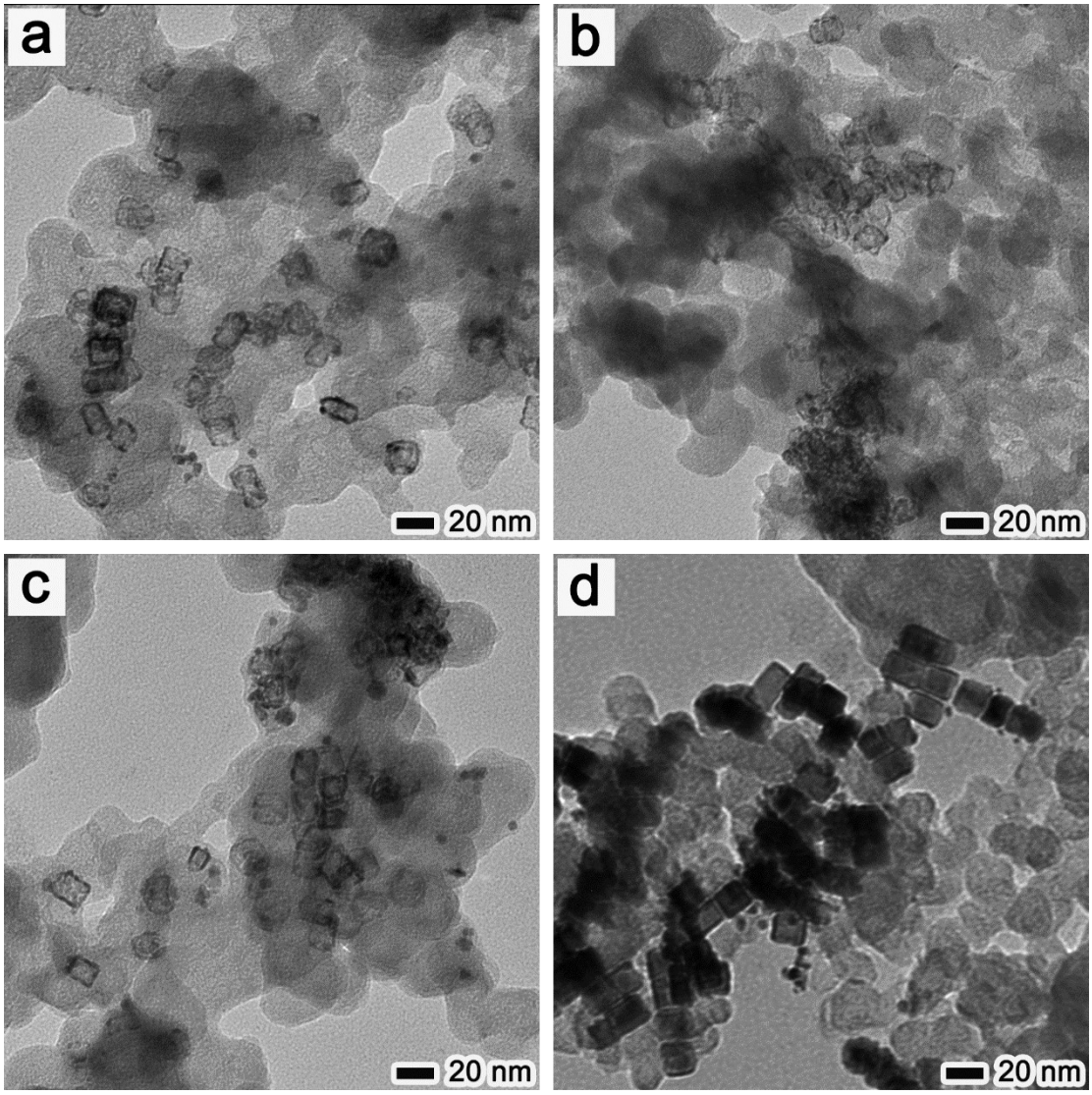

Figure S9. TEM images of (a) $PdPt_{2.5}Ru_{2.4}$/C, (b) $PdPt_{7.3}Ru_{3.6}$/C and (c) $PdPt_{3.7}Ru_{8.1}$/C and Pd@PtRu/C.

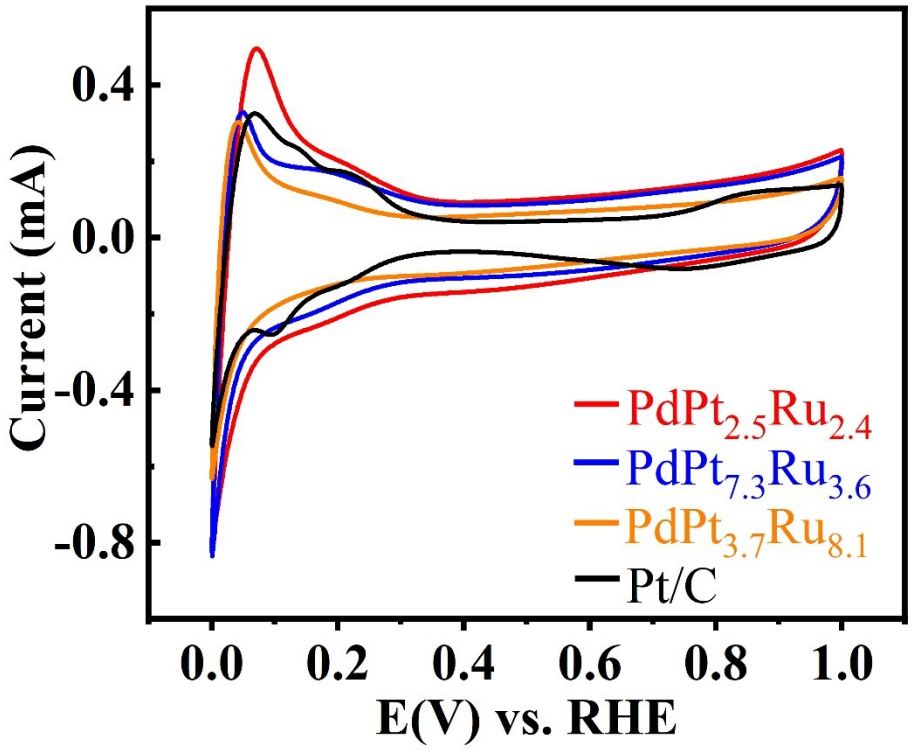

Figure S10. Cyclic voltammetry (CV) curves of $PdPt_{2.5}Ru_{2.4}$/C, $PdPt_{7.3}Ru_{3.6}$/C, $PdPt_{3.7}Ru_{8.1}$/C, commercial Pt/C and commercial PtRu/C catalysts recorded in Ar-saturated 0.1 M $HClO_4$ solution with a scan rate of 100 mV/s.

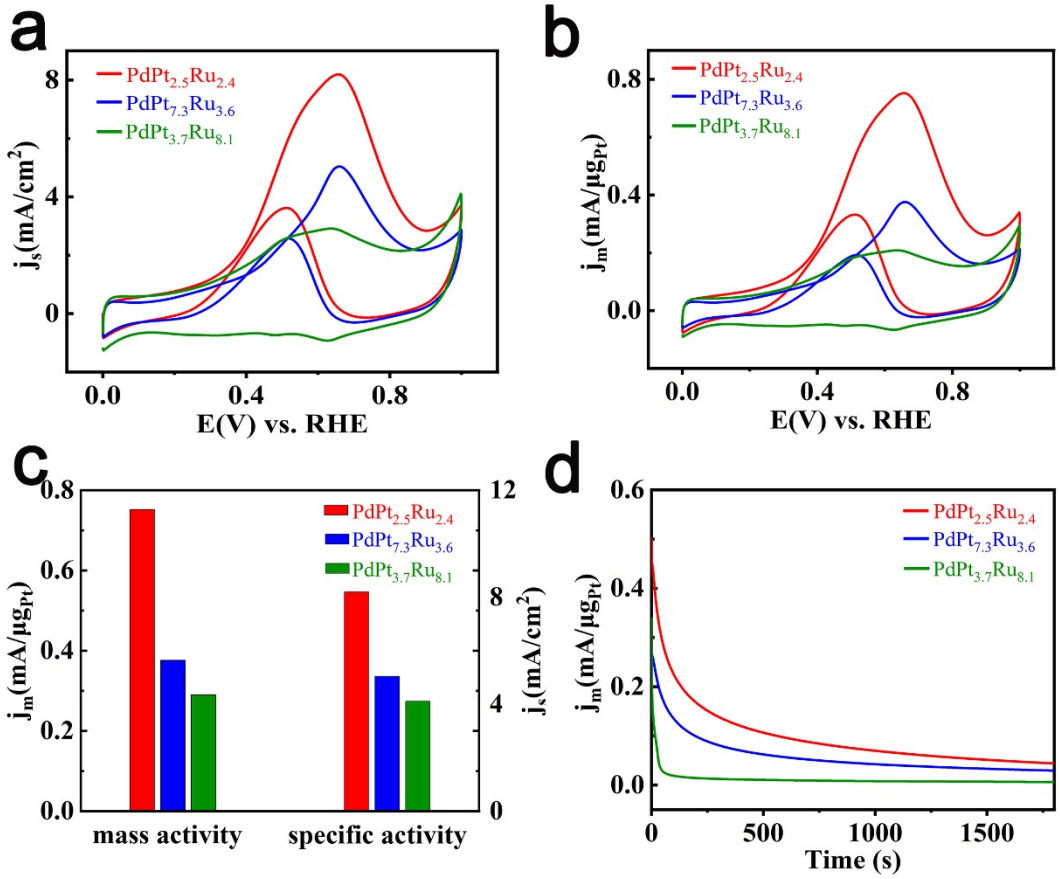

Figure S11. (a, b) Cyclic voltammograms (CVs) of three different catalysts including $PdPt_{7.3}Ru_{3.6}$/C, $PdPt_{2.5}Ru_{2.4}$/C and $PdPt_{3.7}Ru_{8.1}$/C for the MOR normalized by the ECSA and Pt mass, respectively. (c) Specific and mass activity at the peak position of the forward curve. (d) Current–time curves (I–t) for methanol electrooxidation of these three catalysts at the peak position voltage (vs. RHE) for 1800 s.

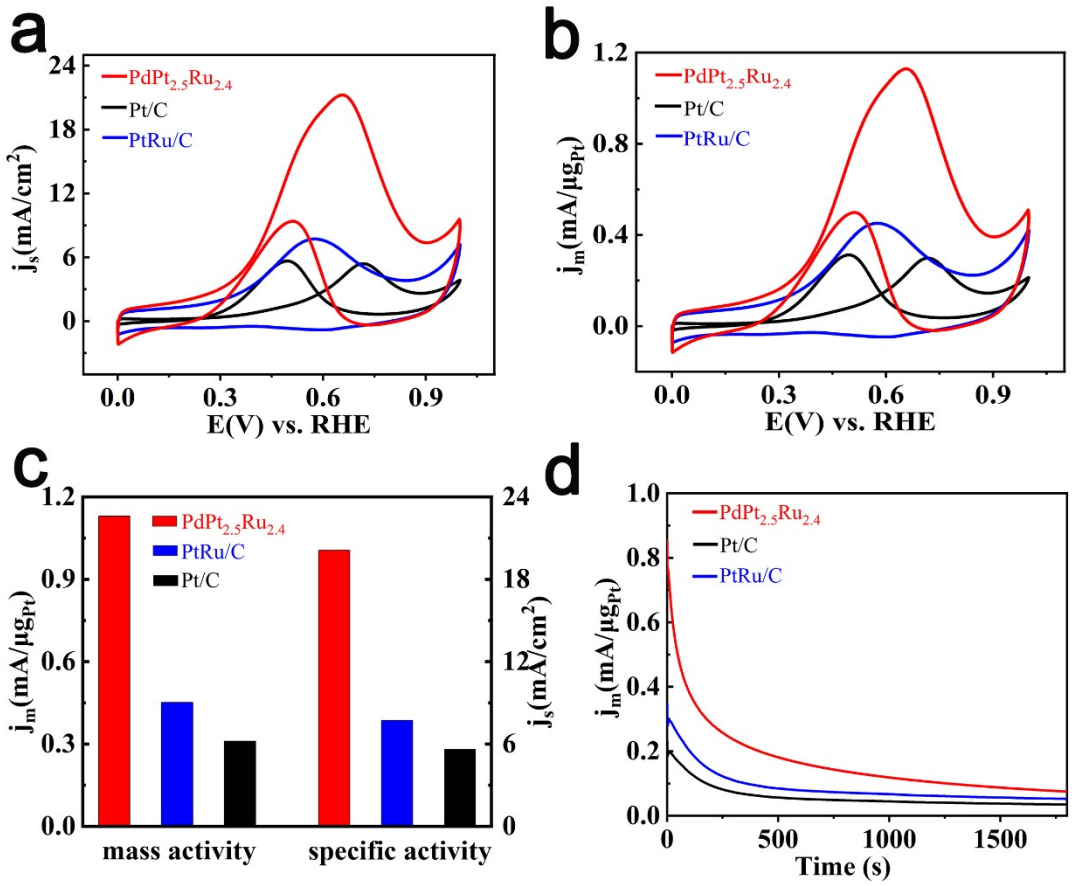

Figure S12. (a, b) Cyclic voltammograms (CVs) of three different catalysts including $PdPt_{2.5}Ru_{2.4}$ nanocages (red), commercial Pt/C (black) and commercial PtRu/C (blue) for MOR in 0.1 M $HClO_4$ and 1 M CH_3OH normalized by the ECSA and Pt mass, respectively. (c) Specific and mass activity at the peak position of the forward curve. (d) Current–time curves (I–t) for methanol electrooxidation of these three catalysts at the peak position voltage (vs. RHE) for 1800 s.

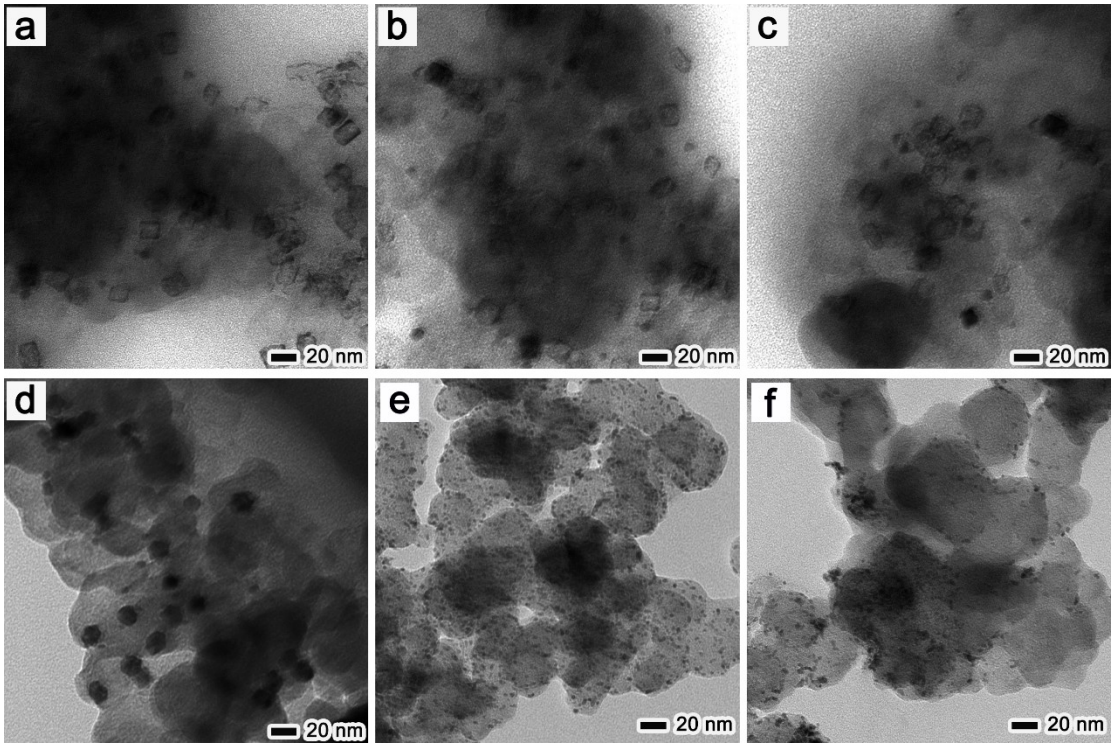

Figure S13. TEM images of (a) $PdPt_{7.3}Ru_{3.6}/C$, (b) $PdPt_{2.5}Ru_{2.4}/C$, (c) $PdPt_{3.7}Ru_{8.1}/C$, (d) Pd@PtRu/C, (e) Pt/C, and (f) PtRu/C after stability test.

Reference

[1] C. Li, X. Chen, L. Zhang, S. Yan, A. Sharma, B. Zhao, A. Kumbhar, G. Zhou, and J. Fang, *Angew. Chem. Int. Ed.*, **2021**, *60*, 7675 – 7680.

[2] B. Sun , L. Huang, S. Su, S. Luo, C. Meng, H. M. A. Basit, J. Xiao, T. Bian, S. Su, *Mater. Chem. Phy.*, **2020**, *252*, 123234.

[3] L. Huang, X. Zhang, Q. Wang, Y. Han, Y. Fang and S. Dong, J. Am. Chem. Soc., **2018**, *140*, 1142–1147.

[4] S. Lu, K. Eid, D. Ge, J. Guo, L. Wang, H. Wang and H. Gu, *Nanoscale*, **2017**, *9*, 1033.

[5] N. Gao, X. Wu, X. Li, J. Huang, D. Li, D. Yang and H. Zhang, *RSC Adv.*, **2020**, *10*, 12689.

[6] P. Yang, X. Yuan, H. Liu, H. Zheng, D. Yang, L. Chen, M. Cao, Y. Xu, Y. Min, Y. Li and Q. Zhang, *Adv. Funct. Mater.*, **2018**, *28*, 1704774.

[7] M. Chen, B. Lou, Z. Ni and B. Xu, *Electrochim. Acta*, **2015**, *165*, 105-109.

[8] L. Huang, W. Zhang, P. Li, Y. Song, H. Sheng, Y. Du, Y. Wang, Y. Wu, X. Hong, Y, Ding, X. Yuan and M. Zhu, *Nano Res.*, **2019**, *5*, 1147-1153.

[9] Y. Zhang, R. Shi, J. Ren, Y. Dai, Y. Yuan and Z. Wang, *Langmuir*, **2019**, *35*, 16752-16760.

[10] P. Wang, Y. Zhang, R. Shi, Z. Wang, *ACS Appl. Energy Mater.*, **2019**, *2*, 2515-2523.

[11] T. Bian, B. Sun, S. Luo, L. Huang, S. Su, C. Meng, S. Su, A. Yuan, H. Zhang, *RSC Adv.*, **2019**, *9*, 35887-35894